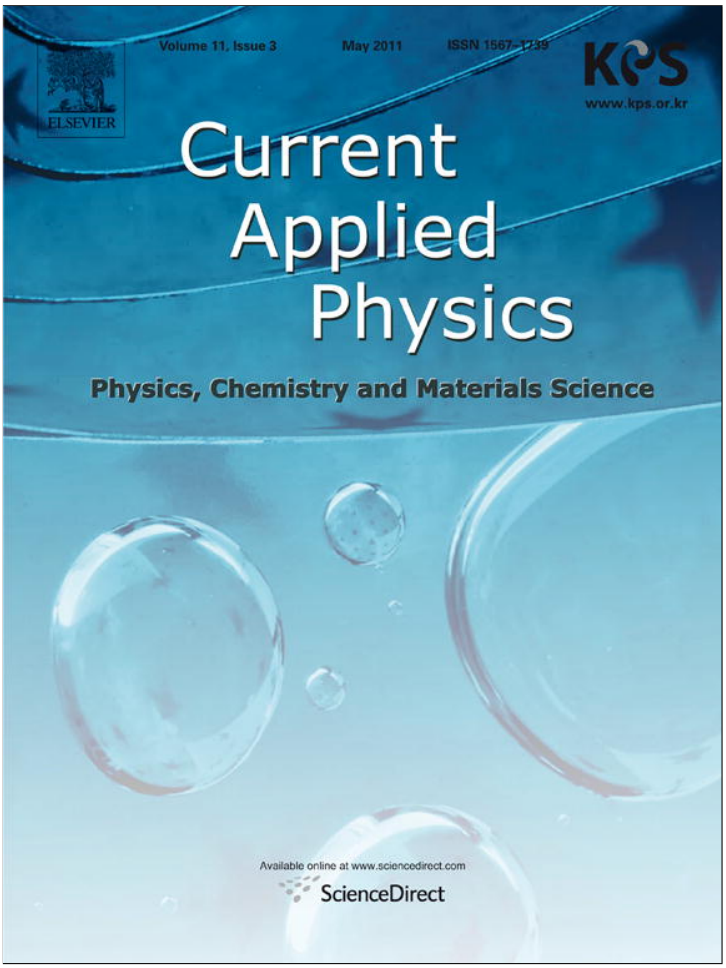

Current Applied Physics 11 (2011) 582–585

Contents lists available at ScienceDirect

Current Applied Physics

journal homepage: www.elsevier.com/locate/cap

Transflective fringe-field switching liquid crystal display using an embedded wire grid polarizer

Miyoung Kim [a], Young Jin Lim [b], Jung Hwa Her [a], Mi-Kyung Kim [a], Zhibing Ge [c], Shin-Tson Wu [c], Seung Hee Lee [a,b,*]

[a] Department of Polymer-Nano Science and Technology, Chonbuk National University, 1Ga 664-14, Deokjin-dong, Deokjin-ku, Jeonju, Jeonbuk 561-756, Republic of Korea
[b] Department of BIN Fusion Technology, Chonbuk National University, 1Ga 664-14, Deokjin-dong, Deokjin-ku, Jeonju, Jeonbuk 561-756, Republic of Korea
[c] College of Optics and Photonics, University of Central Florida, Orlando, FL 32816, United States

ARTICLE INFO

Article history:
Received 13 October 2009
Received in revised form
28 August 2010
Accepted 1 October 2010
Available online 8 October 2010

Keywords:
Transflective liquid crystal display
Fringe-field switching
Wire grid polarizer

ABSTRACT

A single-cell-gap and single-gamma transflective liquid crystal display (TR-LCD) using fringe-field switching is achieved by an embedded wire grid polarizer. In the proposed TR-LCD, the common electrode is patterned into nano-sized wire grids in the reflective part whereas it remains a plane shape in the transmissive part. The nano-sized wire grids play dual roles as common electrode and reflective polarizer in the reflective part. By optimizing the pixel electrode structures, a single gamma curve for the reflective and transmissive parts is demonstrated. Such a TR-LCD is free from in-cell retarder, compensation film, and additional reflector.

1. Introduction

Transflective liquid crystal displays (TR-LCDs) have been widely used in mobile displays because of their readability under any ambient lighting conditions. Recently, several TR-LCDs employing homogenous cells driven either by in-plane switching (IPS) [1–3] or by fringe-field switching (FFS) [4–11] have been reported because they show excellent electro-optic characteristics in the transmissive part. However, to achieve high optical performance in both reflective (R) and transmissive (T) parts several of these devices adopt dual cell gaps in the T and R regions, and compensation films or patterned in-cell retarder (ICR) although it is quite difficult to have an accurate control on the ICR formation. As a result, the manufacturing cost of TR-LCDs remains relatively high and the electro-optic performance still needs further improvement.

In this paper, we propose a TR-LCD driven by fringe electric fields using an embedded wire grid polarizer (WGP) that functions as both reflector and common electrode for the R part. The incident light with electric field vector parallel to the wire grids (say, *s*-wave) is reflected while the perpendicular component (p-wave) is transmitted through the WGP [12,13]. This device concept is useful to make TR-LCDs with single cell gap and single gamma curve. However, in the transflective devices using WGP as a reflector [14] the WGP is formed separately from the pixel or common electrode, which might increase the device thickness due to additional WGP layer and have a complicated cell structure.

To simplify the device structure, we proposed new TR-LCD using WGP which perform role of common electrode and reflector at the same time in the R part. The manufacture of the WGP could easily be included in the manufacturing process of the a-Si:H TFT [15]. In addition, we also propose to utilize patterned common electrodes (rather than the planar one in a typical FFS device) in the T region to match the voltage-dependent transmittance (VT) with the voltage-dependent reflectance (VR) curves. Detailed electro-optic characteristics of the device are discussed as follows.

2. Switching principle and cell condition

Fig. 1 shows the proposed cell structure of the single cell gap TR-LCD associated with the FFS mode using a wire grid polarizer. In the device, pixel and common electrodes exist on the bottom substrate, similar to a conventional transmissive FFS mode. The pixel electrode is patterned with an electrode width (w') and distance (l) between two adjacent stripes, which are 3 μm and 4.5 μm, respectively. The common electrode of the T part is not

* Corresponding author. Department of Polymer-Nano Science and Technology, Chonbuk National University, 1Ga 664-14, Deokjin-dong, Deokjin-ku, Jeonju, Jeonbuk 561-756, Republic of Korea. Tel.: +82 63 270 2343; fax: +82 63 270 2341.
E-mail address: lsh1@chonbuk.ac.kr (S.H. Lee).

1567-1739/$ – see front matter © 2010 Elsevier B.V. All rights reserved.
doi:10.1016/j.cap.2010.10.001

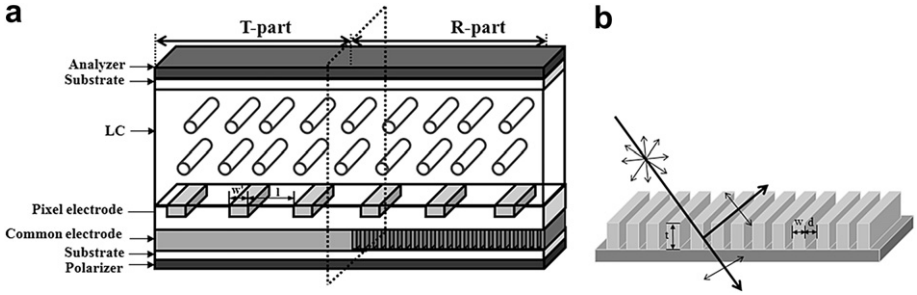

Fig. 1. Proposed TR-LCD cell structure driven by fringe electric field with wire grid polarizer in the reflective part(a) and enlarge view of wire grid polarizer at reflective part of common electrode (b).

patterned but the common electrode of the R part is patterned after that of WGP. The height (t) and width (w) of the WGP are 180 nm and 82 nm, respectively. The WGP is separated at a distance $d = 68$ nm as shown Fig. 1(b). If an unpolarized light impinges on the WGP surface, the light component of electric field vector, parallel to the wire grid will be fully reflected by the WGP. The LC directors are initially homogeneously aligned, the rubbing direction is parallel to the bottom polarizer's axis, and the top analyzer is crossed to the bottom polarizer.

In an FFS cell, the transmittance under two crossed polarizers is described by:

$$T = T_o \sin^2 2\psi(V) \sin^2(\delta/2), \quad (1)$$

where ψ is the angle between the polarizer's transmission axis and the effective LC layer axis, and δ is the phase difference between the ordinary and extraordinary rays, defined by $\delta = 2\pi d\Delta n_{eff}(V)/\lambda$ where d is the LC layer thickness and Δn_{eff} is the voltage-dependent effective birefringence of the LC layer, and λ is the incident wavelength.

Fig. 2 shows the polarization path on the Poincare sphere. P1 and P2 indicate the transmission axes of polarizer and analyzer, respectively. At the voltage-off state of the R part, the linearly polarized light comes through the analyzer's transmission axis at P2 in Fig. 2(a) and propagates along the slow axis of the LC director without changing its polarization state. Finally, this linearly polarized light transmits through the WGP. As a result, the light is absorbed by the polarizer (whose absorption axis is also at P2) to appear black in the R region. In the voltage-off state of the T part, the linearly polarized light comes through the polarizer at P1 and then passes through the LC layer without changing its polarization state. Thus it is blocked by the analyzer (whose absorption axis is also at P1), showing a dark state as well. The device is realized as a normally black mode in both R and T parts, as depicted in Fig. 2(a). It is expressed by black spot on the Poincaré sphere. In the presence of electric fields, the cell is designed for the LC director to have an average twist angle of nearly 45° in both R and T parts, so that maximum reflectance and transmittance can be achieved. Under such a circumstance, the linearly polarized light is rotated by 90° in the R and T parts, as shown in Fig. 2(b) and (c). Fig. 2(b) and (c) just illustrate the light polarization traces by assuming the bright state LC director profile is like an effective $\lambda/2$ plate with its effective optic axis at 45° away from the its original alignment. The real polarization change in the bright state of an FFS cell could be found in Reference [16].

In order to calculate electro-optic characteristics of the device, commercially available software "LCD master" (Shintech, Japan) is employed. The LC material is a TFT-grade mixture with parameters listed as following: dielectric anisotropy $\Delta\varepsilon = +8.2$, elastic constants $K_1 = 9.7$ *pN*, $K_2 = 5.2$ *pN*, and $K_3 = 13.3$ *pN*. The LC surface tilt angle is 2° and the LC layer thickness is 4 μm in both T and R regions. The angle between lengthwise direction of the pixel electrode stripes and the LC rubbing direction is 15°. Here, a 2 × 2 extended Jones matrix was adopted to calculate the reflectance and transmittance [17]. The transmittance of two parallel polarizers is calculated to be 35%.

3. Results and discussion

At first, the optimal cell retardation for maximizing reflectance and transmittance is calculated as a function of $d\Delta n$. As indicated in Fig. 3, the maximum transmittance (T_{max}) is rather insensitive to the variation of $d\Delta n$ while the maximum reflectance (R_{max}) is achieved at $d\Delta n = 0.42$ μm. By choosing $d\Delta n = 0.42$ μm, T_{max} and R_{max} were found to be 30% and 27%, respectively. The optical efficiency in reflective area exceeds 77%. In the simulation, we assume the reflectance of WGP to be 100% for an incident linearly polarized light at normal direction. However, it was reported that reflectance of the fabricated WGP was over 78%, which is close to the reflectance of an aluminum mirror [18]. In addition, the operating voltage (V_{op}) for both R and T parts was 4.2 V_{rms}. The reason for the same

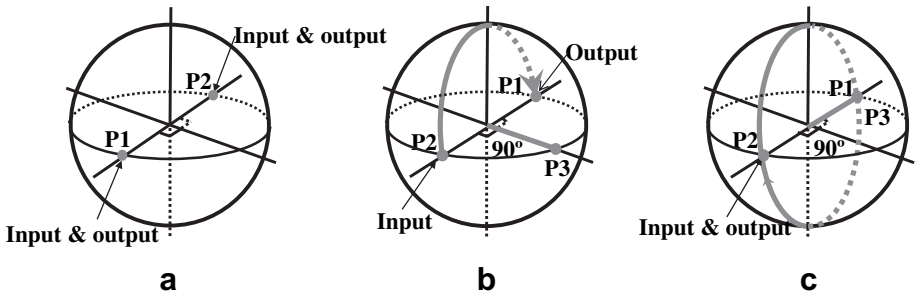

Fig. 2. Poincaré sphere representation of the polarization paths of (a) dark states in both T and R parts, and white state in (b) T part and (c) R part, respectively.

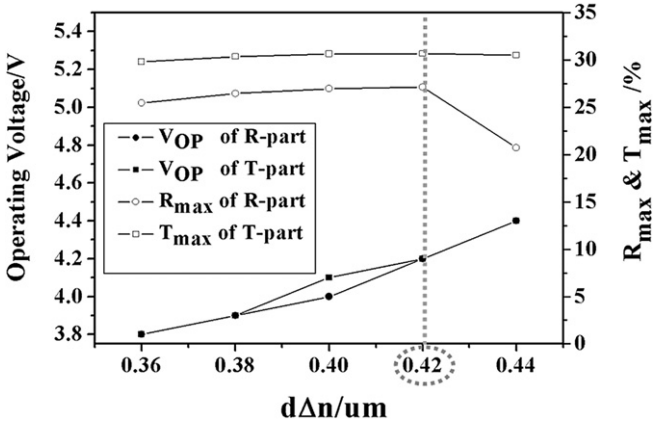

Fig. 3. The operating voltages and maximum reflectance and transmittance in each area as a function of $d\Delta n$.

operating voltage in both areas comes from the fact that both T and R parts require the LC layer to be an equivalent λ/2 plate for achieving maximum light efficiency.

With these cell parameters, we then calculate VR and VT curves as shown in Fig. 4. Unfortunately, the two curves do not overlap perfectly although the V_{op} are the same. The main discrepancy originates from the different threshold voltages of the T and R parts because the electric field intensity is different between the R and T parts due to use of WGP in the R area. The field intensity near electrode surface to rotate the LC in T part is stronger than that in the R Part so that threshold voltage of the T part is much lower than that in the R part as shown in Fig. 4.

At an intermediate gray level, the incident light reaching the WGP surface is elliptically polarized. Thus only the *s*-wave parallel to the wire grids will be reflected back to viewer and the remaining *p*-wave penetrates the WGP and becomes lost. Therefore, as compared to the T part, this additional light loss at the WGP surfaces makes the VR always below the VT curves in intermediate gray levels, except the dark and full bright states. Hence further optimization in the device structure is required to match both the curves so that it can be driven using a single gamma curve.

In order to achieve a single gamma curve, the electric field in the T part is required to be reduced to shift the VT curve toward the high voltage direction. Hence we improved the proposed device by patterning the common electrode [19] in the T part as shown in Fig. 5. With patterned structure, the horizontal distance (l') between pixel and common electrodes appears with another electrode width (w'') of common electrode. As l' increases, the intensity of horizontal electric fields to rotate the LC directors will be decreased as compared to that in non-patterned case when a same voltage is applied. Therefore, having l' between two electrodes will increase the threshold voltage of the T part so that the VT curve can be shifted to match the VR curve. A series of VT curves are calculated by varying l' from 6 to 3 μm while keeping $w'' = 3$ μm in the T part, as shown in Fig. 6. The threshold voltage decreases with decreasing l' and they overlap with each other perfectly showing a single gamma curve for $l' = 3$ μm in the T part.

Additionally, to obtain wide viewing angle characteristic it is important to confirm the polarized - reflectance and - transmittance of WGP as a function of the incident angle. It depends on the configuration of the wire grid and numerical aperture. Details of the investigation are discussed in references [13,20]. The performance of WGP is best when patterned direction of metal and plane of incidence is the same and numerical aperture is lager. Accordingly, to obtain high performance, the physical parameters such as d, grating period ($w + d$), the aperture ratio ($d/w + d$), t, and the properties of the grating metal of the WGP should be optimized.

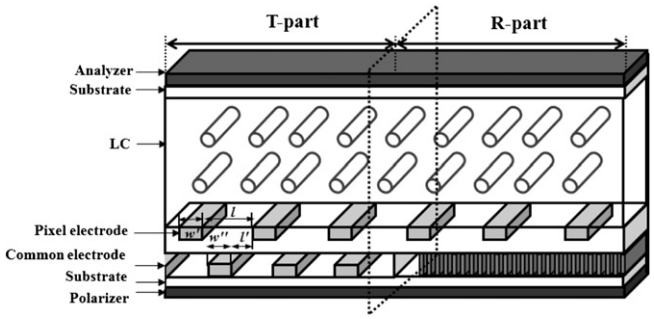

Fig. 5. Cell structure of FFS mode with patterned common electrode.

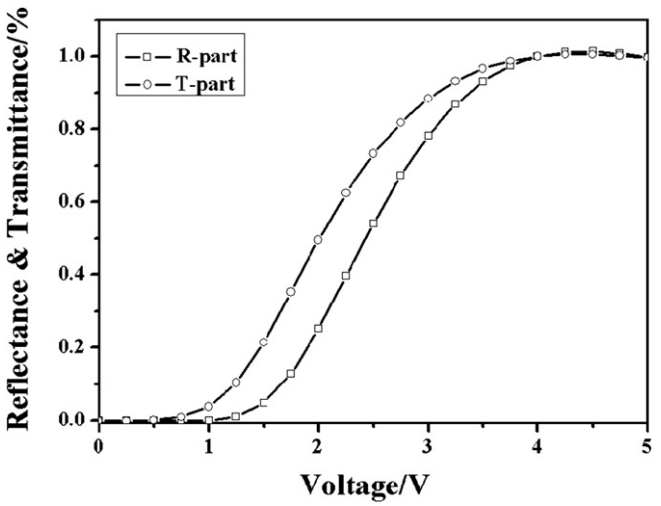

Fig. 4. Normalized VR and VT curves.

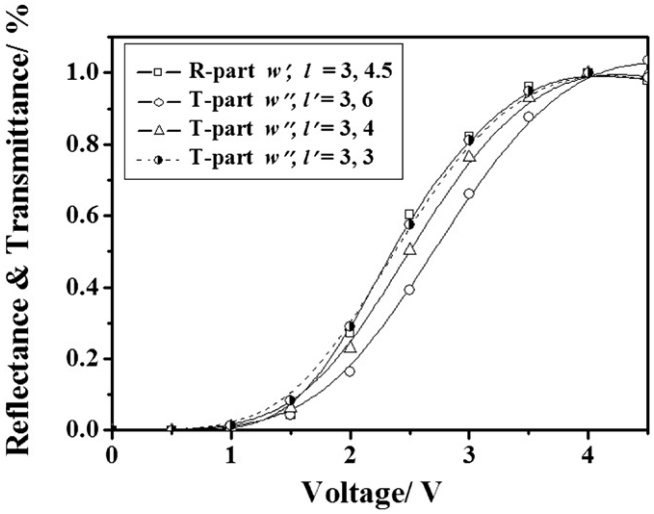

Fig. 6. Normalized VR and VT curves according to the electrode structure of patterned common electrodes.

4. Conclusion

We have proposed a single cell gap and single gamma transflective LCD associated with FFS mode using a wire grid polarizer. In the device, the common electrode is patterned as nano-sized wire grids in the R part whereas it has a plane shape in the T part. To obtain single gamma curve, the pixel electrode structure and rubbing angle are optimized and this device shows both high light efficiency and wide viewing angle. In addition, the device has simple and thin cell structure which does not require any in-cell retarder, compensation film, and reflector, making it a promising candidate for mobile displays.

Acknowledgements

This work was supported by WCU program through MEST (R31-2008-000-200029-0).

References

[1] G.D. Lee, G.H. Kim, S.H. Moon, J.D. Noh, S.C. Kim, W.S. Park, T.H. Yoon, J.C. Kim, S.H. Hong, S.H. Lee, Jpn. J. Appl. Phys. 39 (2000) 221.
[2] J.H. Song, S.H. Lee, Jpn. J. Appl. Phys. 43 (2004) 1113.
[3] K. Park, Y.J. Ko, J.S. Gwag, M. Oh, J.C. Kim, T. Yoon, Mol. Cryst. Liq. Cryst. 434 (2005) 79.
[4] S.H. Lee, S.H. Hong, H.Y. Kim, G.-D. Lee, T.-H. Yoon, Jpn. J. Appl. Phys. 40 (2001) 5334.
[5] T.B. Jung, J.C. Kim, S.H. Lee, Jpn. J. Appl. Phys. 42 (2003) 464.
[6] T.B. Jung, J.H. Song, D.S. Seo, S.H. Lee, Jpn. J. Appl. Phys. 43 (2004) 1211.
[7] Y.J. Lim, J.H. Song, S.H. Lee, Jpn. J. Appl. Phys. 43 (2004) 972.
[8] J.H. Song, Y.J. Lim, M.-H. Lee, S.H. Lee, S.T. Shin, Appl. Phys. Lett. 87 (2005) 011108.
[9] Y.J. Lim, M.-H. Lee, G.-D. Lee, W.-G. Jang, S.H. Lee, J. Phys. D: Appl. Phys. 40 (2007) 2759.
[10] H. Imayama, J. Tanno, K. Igeta, M. Morimoto, S. Komura, T. Nagata, O. Itou, S. Hirota, Soc. Inf. Display Tech. Digest 38 (2007) 1651.
[11] Z. Ge, S.T. Wu, S.H. Lee, Opt. Lett. 33 (2008) 2623.
[12] J. Wang, L. Chen, X. Liu, P. Sciortino, F. Liu, F. Walters, X. Deng, Appl. Phys. Lett. 89 (2006) 141105.
[13] X.J. Yu, H.S. Kwok, J. Appl. Phys. 93 (2003) 4407.
[14] Z. Ge, T.X. Wu, S.T. Wu, Appl. Phys. Lett. 92 (2008) 051109.
[15] J.H. Oh, D.H. Kang, W.H. Park, H.J. Kim, S.M. Hong, J.H. Hur, J. Jang, Soc. Inf. Display Tech. Digest 38 (2007) 1164.
[16] I.H. Yu, I.S. Song, J.Y. Lee, S.H. Lee, J. Phys. D: Appl. Phys. 39 (2006) 2367.
[17] A. Lien, Appl. Phys. Lett. 57 (1990) 2767.
[18] T. Sergan, J. Kelly, M. Lavrentovich, E. Gardner, R. Perkins, J. Hansen, R. Critchfield, Soc. Inf. Display Tech. Digest 33 (2002) 514.
[19] Y.H. Jeong, Y.J. Lim, E. Jeong, W.G. Jang, S.H. Lee, Liq. Cryst. 2 (2008) 187.
[20] X.J. Yu, H.S. Kwok, Soc. Inf. Display Tech. Digest 34 (2003) 878.